

Cite this: *RSC Adv.*, 2017, 7, 17332

Received 2nd February 2017

Accepted 13th March 2017

DOI: 10.1039/c7ra01372h

rsc.li/rsc-advances

## Evaluating the performance of MoS<sub>2</sub> based materials for corrosion protection of mild steel in an aggressive chloride environment†

S. ArunKumar, V. Jegathish, R. Soundharya, M. JesyAlka, C. Arul, S. Sathyanarayanan and Sundar Mayavan\*

In this work for the first time, metal doped (Fe, Co, Ni) MoS<sub>2</sub> sheets dispersed in sunflower oil were explored as a coating for inhibiting Fe metal corrosion in a sodium chloride (NaCl) solution. The incorporation of Fe, Co, and Ni ions resulted in an appreciable increase in the corrosion resistance properties of MoS<sub>2</sub>.

Exposure of metals to environmental and service conditions often results in failure due to oxidation and corrosion. Various types of coatings based on ceramics, metals, and polymers have been used for corrosion protection.<sup>1–3</sup> Organic/polymer coatings can be easily formulated and find wide applications in various industries. However, the main issue with polymeric coatings is the presence of pores/pinholes that lead to the corrosion of the underlying metal substrate. Recently, nanomaterials (as fillers) have shown to significantly improve the corrosion resistance of the polymeric coatings. Among nanomaterials, graphene is believed to be an ideal material for metal protection due to its high impermeability to gases and moisture.<sup>4–6</sup> However, the main issue with graphene is its ability to form a galvanic cell with underlying metals, promoting oxidation/corrosion in the long term.<sup>7</sup> Hence, exploring substitute materials akin to graphene is an area of current research.

MoS<sub>2</sub> is a better alternative to graphene as it has desirable properties similar to graphene, and being a semiconductor it does not form (or enhance) a galvanic cell with underlying metals. In addition, MoS<sub>2</sub> is a phosphorescent material and has greater thermal/chemical stability and lubricity.<sup>8,9</sup> Doping MoS<sub>2</sub> with metals (like cobalt, iron, selenium, *etc.*) results in the formation of a Mo-metal-S phase, which significantly alters/modifies the electronic, chemical and surface properties of MoS<sub>2</sub> for various applications. Fe doped MoS<sub>2</sub> shows enhanced conductivity and catalytic activity compared to pristine MoS<sub>2</sub>.<sup>10</sup> Co doped MoS<sub>2</sub> nanosheets showed enhanced catalytic activity for hydrogen evolution than pristine MoS<sub>2</sub>.<sup>11</sup> Doping with metals like Fe, Co, Ni improved the surface area of MoS<sub>2</sub>.<sup>10,11</sup> Most of the reported work focuses on the utilization of metal doped MoS<sub>2</sub> for catalytic/electronic applications. But to the best of our knowledge pristine

MoS<sub>2</sub>/metal doped MoS<sub>2</sub> has not been explored for corrosion control applications. In this work, for the first time metal doped (Fe, Co, Ni) MoS<sub>2</sub> sheets dispersed in oil were explored as a coating for inhibiting mild steel (Fe) corrosion in a sodium chloride (NaCl) solution. Sunflower oil is used as the binder to increase the adhesion of MoS<sub>2</sub> flakes with the steel surfaces. The incorporation of Fe, Co, and Ni ions resulted in an appreciable increase in the corrosion resistance properties of MoS<sub>2</sub>.

Fe, Co and Ni containing MoS<sub>2</sub> nanosheets were prepared *via* thermal treatment involving MoS<sub>2</sub> (commercially sourced), glycine and metal nitrate (see Experimental in the ESI†). The XRD pattern of pristine MoS<sub>2</sub> and as-prepared Fe–MoS<sub>2</sub>, Co–MoS<sub>2</sub>, Ni–MoS<sub>2</sub> are shown in Fig. S1a†. All peaks can be assigned to hexagonal MoS<sub>2</sub>. After metal (Fe, Co and Ni) doping, all peaks slightly shifted toward smaller diffraction angles (Fig. S1b†), indicating that there is an increase in the interplanar distance. Besides, it is also clear that the XRD peaks of the metal-doped MoS<sub>2</sub> are broader and weaker in intensity, indicating the reduction of the average grain size/crystallinity and an increase of defective and disordered structures in the MoS<sub>2</sub> due to metal doping. No peaks relating to Fe, Co, Ni are evident which is in line with the previously reported Co/Fe/Ni containing MoS<sub>2</sub> compounds.<sup>11</sup> This is an indication that Co/Fe/Ni species are chemically coordinated to the MoS<sub>2</sub> phase. XPS data confirms the presence of Mo, S, O, N, C and metallic species (Fig. S1c†). The morphology and structure of the as-prepared composites were examined by transmission electron microscopy (TEM). Pristine MoS<sub>2</sub> sample have an irregular layered sheet like structure. Addition of metals (to pristine MoS<sub>2</sub>) seems to have significant influence on the surface morphology (Fig. 1). Incorporation of Fe, Co and Ni resulted in an appreciable increase in the porosity of the film (Fig. 1b–d). Field emission scanning electron microscopy (FE-SEM) images of Fe–MoS<sub>2</sub> (Fig. S2a†) showed the clear presence of large number of pores (around hundreds of nanometres) along the entire structure, possibly formed due to the gas evolution by

CSIR-Central Electrochemical Research Institute, Corrosion and Materials Protection Division, Karaikudi – 630006, Tamil Nadu, India. E-mail: sundarmayavan@cecri.res.in

† Electronic supplementary information (ESI) available. See DOI: 10.1039/c7ra01372h



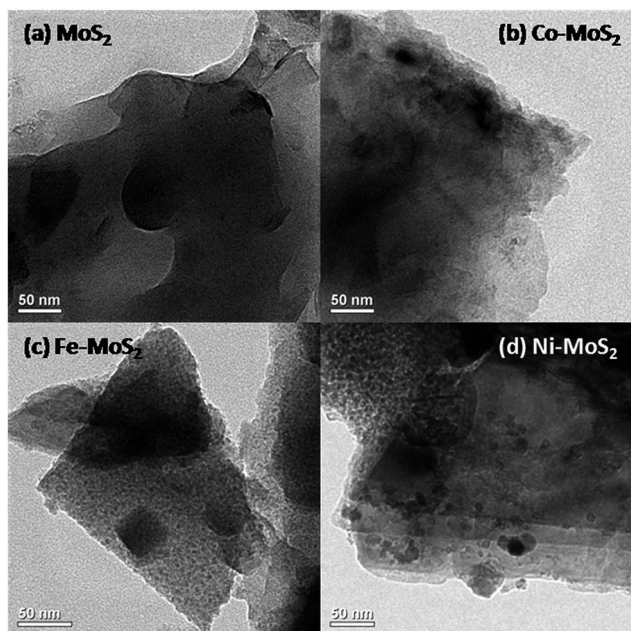


Fig. 1 TEM images of (a) MoS<sub>2</sub>, (b) Co-MoS<sub>2</sub>, (c) Fe-MoS<sub>2</sub> and (d) Ni-MoS<sub>2</sub>.

glycine–nitrate decomposition during synthesis process. But pristine MoS<sub>2</sub> shows non-porous sheet like structures (with no pores) (Fig. S2b†). XRF was used to further verify the composition of MoS<sub>2</sub> samples. XRF data indicates the presence of Mo, S, O along with corresponding metallic species (Fig. S3†).

The as-prepared MoS<sub>2</sub> and metal doped MoS<sub>2</sub> powders are dispersed in sunflower oil under sonication to form a MoS<sub>2</sub>-based coating solution (MOC) (see Experimental in ESI†). XRD pattern of the MoS<sub>2</sub>-oil coated samples is shown in Fig. 2. Most of the diffraction originating from the (100), (101), (103), (105) and (110) planes of the bulk MoS<sub>2</sub> (Fig. S1†) are completely absent except the low intensity broad (002) peak at around 15°, indicating that the oil sheets. The additional diffraction peak at 45° and 20° originates from the Fe substrate and oil crystallization.<sup>12</sup> The surface morphology of the MOC coated samples

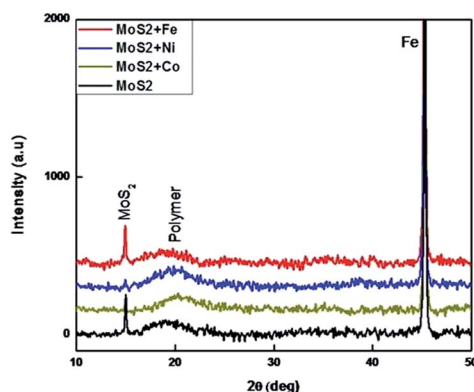


Fig. 2 XRD pattern of MoS<sub>2</sub> and metal doped MoS<sub>2</sub>-oil coated on Fe samples.

were examined by SEM. SEM and AFM images (Fig. S4†) show the smooth morphology of the coating surface without any nanostructures.

Open circuit voltage (OCV) measurements of MOC coated Fe samples in 3.5% sodium chloride (NaCl) solution are shown in Fig. 3. As a reference the OCV curve of Fe is also displayed. OCV values shows that all samples are nobler than the bare Fe (Fig. 3). For metal doped MoS<sub>2</sub> the potential was shifted to more noble direction (ennobling). The observed ennobling is an indication of passivation. Coating with pristine MoS<sub>2</sub> and MoS<sub>2</sub>-Co does not show any influence of the steel substrate at test duration (as there is no significant change in the OCV values for the test duration). For the Ni and Fe the influence of underlying Fe substrate (change in the OCV values) can be observed at test duration. Potentiodynamic polarization measurements in 3.5% NaCl solution of MOC on Fe substrates are plotted in Fig. 3b. As a reference the curve of Fe is also displayed. Table 1 shows the corrosion protection performance of MOC in 3.5% NaCl solution.  $E_{\text{corr}}$  values shows that all samples are nobler than the bare Fe. With the addition of metals the corrosion potential was shifted to more noble direction (ennobling). A maximum  $E_{\text{corr}}$  value of 0.279 V was obtained for the MoS<sub>2</sub>-Fe coated sample. The  $I_{\text{corr}}$  value decreases from 83.66  $\mu\text{A cm}^{-2}$  corresponding to the mild steel to 0.001  $\mu\text{A cm}^{-2}$  in the case of MoS<sub>2</sub>-Fe coating. The corrosion protection efficiency deduced from measured  $I_{\text{corr}}$  value is shown in Table 1. The protection efficiency is about 99% for MOC coatings. Among various metals Fe shows the highest protection efficiency with low  $I_{\text{corr}}$  and high  $E_{\text{corr}}$  values. Bode plots corresponding to MOC (shown in Fig. 4) proved that the

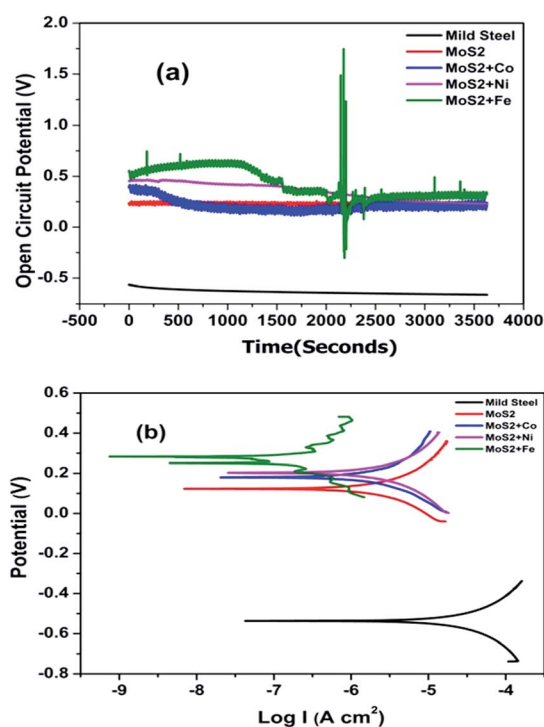
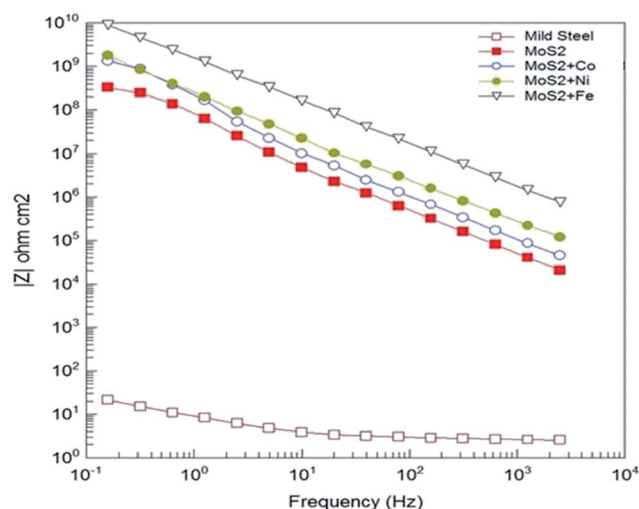


Fig. 3 OCV (a) and polarization curves (b) of MOC on Fe at 25 °C.



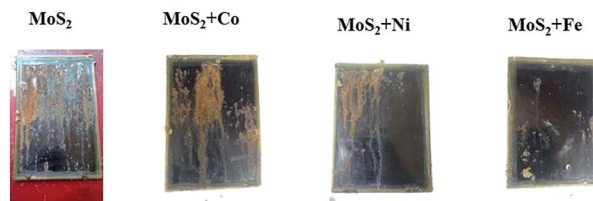
**Table 1** Corrosion protection performance of MOC in 3.5% NaCl solution

S. No	Sample name	$E_{\text{corr}}$ (V)	$I_{\text{corr}}$ $\mu\text{A cm}^{-2}$	Protection efficiency (%)
1	Mild steel	−0.536	83.66	—
2	MoS <sub>2</sub>	0.149	0.005	99.993
3	MoS <sub>2</sub> + Co	0.180	0.003	99.996
4	MoS <sub>2</sub> + Ni	0.209	0.002	99.997
5	MoS <sub>2</sub> + Fe	0.279	0.001	99.998

**Fig. 4** Impedance spectra of MOC.

coating is highly capacitive. The slope of the high-frequency data is an indication of the mechanism of coating degradation. A slope of  $-1$  over the entire spectrum indicates capacitive behaviour, whereas a slope of  $-1/2$  is an indication of diffusion control leading to substrate corrosion. From the Bode plot it is observed that MoS<sub>2</sub>/Fe oil coating showed a high impedance of  $>10^{10}$  ohm  $\text{cm}^{-2}$ , as compared MoS<sub>2</sub>/Co, MoS<sub>2</sub>/Ni and MoS<sub>2</sub> oil coating. Fig. S5† shows Nyquist plots of bare Fe and MOC in NaCl. The plot for bare Fe exhibits semicircular characteristics with low resistivity to the corrosive medium. The MoS<sub>2</sub> based coatings provides a clear indication about capacitive behaviour, consistent with an intact coating in the absence of defects. The prepared coating shows much better anticorrosion properties than graphene and conducting polymer based coatings in terms of OCV and impedance values.<sup>13–16</sup> The coating resistance of the as-prepared oil coating is at least 2 orders of magnitude higher than observed with conducting polymer based coatings and graphene based coatings.<sup>13,14</sup>

Salt spray test was conducted as per ASTM B117 to test the stability of the coatings. After 74 hour, MoS<sub>2</sub>/Co, MoS<sub>2</sub>/Fe, MoS<sub>2</sub>/Ni, MoS<sub>2</sub>/Zn and MoS<sub>2</sub>/Mn oil coated sample starts to form rust. After 124 hour, MoS<sub>2</sub>/Fe oil coated sample showed a less percentage in corrosion over the metal surface and remaining coated sample gets mostly corroded (Fig. 5). From the salt spray test, we can conclude that MoS<sub>2</sub>/Fe shows a superior

**124 HOURS****Fig. 5** Salt spray analysis of MOC on Fe after 124 hours.

anticorrosion protection to the Fe. Contact angle (Fig. S6†) for the MOC coatings was taken and it was observed that the coated material showed a hydrophobic nature. Contact angle for MoS<sub>2</sub>/Fe (84.4°), MoS<sub>2</sub>/Ni (82.1°) MoS<sub>2</sub>/Co (81.4°) and for MoS<sub>2</sub> (78.5°). The adhesion test was done over the coating surface by cross cut square lattice from the substrate surface and the edges are completely smooth and satisfied with ASTM D3359 scale. To understand the abrasion resistance of the coatings, the coated surface was abraded by using two rotating wheels of 500 g load. The coated sample withstands more than 1000 cycles indicating excellent abrasion resistance.

In conclusion, for the first time a MoS<sub>2</sub> based oil coatings has been successfully tested for its metallic corrosion resistance under aggressive chloride ion conditions. Metal containing MoS<sub>2</sub> coatings showed better corrosion protection properties as compared to pristine MoS<sub>2</sub> materials.

**Notes and references**

- 1 H. Jensen and G. Sorensen, *Surf. Coat. Technol.*, 1996, **84**, 500.
- 2 T. K. Rout, G. Jha, A. K. Singh, N. Bandyopadhyay and O. N. Mohanty, *Surf. Coat. Technol.*, 2003, **167**, 16.
- 3 A. K. Satapathy, G. Gunasekaran, S. C. Sahoo, K. Amit and P. V. Rodrigues, *Corros. Sci.*, 2009, **51**, 2848.
- 4 R. K. Singh Raman, P. C. Banerjee, D. E. Lobo, H. Gullapalli, M. Sumandasa, A. Kumar, L. Choudhary, R. Tkac, P. M. Ajayan and M. Majumder, *Carbon*, 2012, **50**, 4040.
- 5 N. T. Kirkland, T. Schiller, N. Medhekar and N. Birbilis, *Corros. Sci.*, 2012, **56**, 1.
- 6 S. Mayavan, T. Siva and S. Sathiyarayanan, *RSC Adv.*, 2013, **3**, 24868.
- 7 M. Schriver, W. Regan, W. J. Gannett, A. M. Zaniwski, M. F. Crommie and A. Zettl, *ACS Nano*, 2013, **7**, 5763–5768.
- 8 G. Zhang, H. Liu, J. Qu and J. Li, *Energy Environ. Sci.*, 2016, **9**, 1190.
- 9 I. Song, C. Park and H. C. Choi, *RSC Adv.*, 2015, **5**, 7495–7514.
- 10 D. Ma, Y. Tang, G. Yang, J. Zeng, C. He and Z. Lu, *Appl. Surf. Sci.*, 2015, **328**, 71.
- 11 X. Dai, K. Du, Z. Li, M. Liu, Y. Ma, H. Sun, X. Zhang and Y. Yang, *ACS Appl. Mater. Interfaces*, 2015, **7**, 27242.
- 12 T. Balakrishnan, S. Sathiyarayanan and S. Mayavan, *ACS Appl. Mater. Interfaces*, 2015, **7**, 19781.



- 13 S. Sathiyarayanan, S. Muthkrishnan and G. Venkatachari, Corrosion Protection of Steel by Polyaniline Blended Coating, *Electrochim. Acta*, 2006, **51**, 6313.
- 14 S. Mayavan, T. Siva and S. Sathiyarayanan, *RSC Adv.*, 2013, **3**, 24868.
- 15 E. Owczare and L. Adamczyk, *J. Appl. Electrochem.*, 2016, **46**, 635.
- 16 S. Radhakrishnan, N. Sonawane and C. R. Siju, *Prog. Org. Coat.*, 2009, **64**, 383.

